Annual Symposium of the Hellenic Nuclear Physics Society

Τόμ. 13 (2004)

HNPS2004

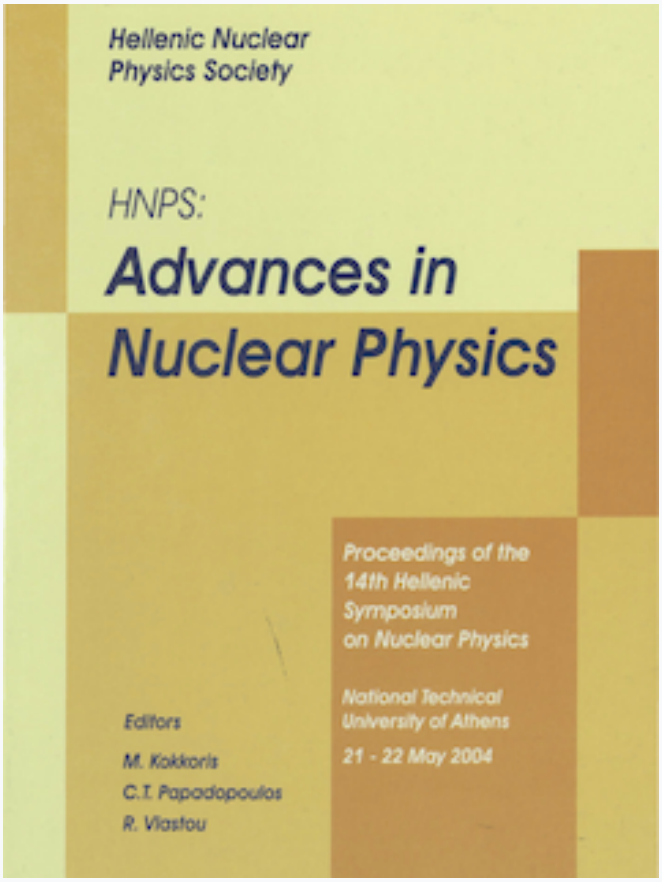

Searching for a Global alpha-nucleus Potential for Astrophysical Applications

A. Spyrou, A. Lagoyannis, Ch. Zarkadas, S. Harissopulos, H.-W. Becker, C. Rolfs, P. Demetriou

doi: 10.12681/hnps.2967

Searching for a Global alpha-nucleus Potential for Astrophysical Applications

A. Spyrou [a], A. Lagoyannis [a], Ch. Zarkadas [a], S. Harissopulos [a], H.-W. Becker [b], C. Rolfs [b], P. Demetriou [c, 1]

[a] *Institute of Nuclear Physics, NCSR Demokritos, POB 60228, 153.10 Aghia Paraskevi, Athens, Greece.*

[b] *Institut fur Experimentalphysik III, Ruhr-Universität- Bochum, Universitatsstrasse 150, 40781 Bochum, Germany.*

[c] *Institute d'Astronomie et d'Astrophysique, Université Libre de Bruxelles, CP226, Campus de la Plaine, 1050 Brussels, Belgium.*

Abstract

This contribution reports on a systematic investigation of in-beam cross-section measurements of (α, γ) reactions, carried out using a 4π calorimeter. The results are compared to the predictions of the Hauser–Feshbach (HF) theory. This comparison puts some constraints on the relevant nuclear properties entering the HF calculations.

1 Introduction

The term "p nuclei" refers to 35 proton-rich nuclei, heavier than iron, which are synthesized in the cosmos via a special nucleosynthetic mechanism known as the p process [1]. The p process involves a series of (γ, n), (γ, p), (γ, α) reactions and their inverse. The origin of the p nuclei is a major problem in stellar-nucleosynthesis models due to the discrepancies between observed and calculated p-nuclei abundances. These discrepancies could be attributed to uncertainties in the description of the astrophysical processes involved and/or to uncertainties in the nuclear physics properties entering the abundance calculations. The latter are based on extended nuclear reaction network calculations involving almost 20000 reactions. As it is hardly possible to have experimental data on all these cross sections at astrophysicaly relevant energies, abundance calculations have to rely almost completely on the predictions of the HF theory. Therefore, through comparisons with experimental data, the reliability of

[1] Present address: *INP, NCSR "Demokritos", Athens, Greece.*

the latter (HF) calculations has to be checked independently (via cross section measurements) since they may strongly affect the p-nuclei abundance calculations. This work reports on a series of in-beam cross section measurements of (α, γ) reactions at energies of astrophysical interest. The data are compared with the Hauser-Feshbach predictions obtained with the statistical-model code MOST [2].

2 Experimental Setup

All measurements were carried out at the 4 MV Dynamitron Tandem accelerator of the Ruhr-Universität Bochum, Germany. The energy of the alpha beam varied from 9.5 to 11.5 MeV. Experimental details on the reactions studied are presented in table 1. The thickness of the targets listed in this table was determined by XRF measurements with an accuracy of 6%. The targets were cooled with air during all runs. After impinging on the target, the beam was stopped by a thick Ta foil placed at a distance of 2 m away from the target. This way, the contribution from disturbing gamma rays, coming from reactions of the alpha beam with the surrounding materials, was significantly reduced. In addition, blocks of paraffin covered with Cd foils were placed around the beam stopper for the reduction of the neutron flux arising mainly from (a,n) reactions. A high efficiency γ-ray detector consisting of a 12"x12" NaI(Tl) single crystal (BICRON) with a bore hole along its axis was used [3]. The targets were placed at the center of the detector so that a solid angle of almost 4π was covered. The energy resolution of the 4π detector was 2% for a 10 MeV γ ray. The absolute efficiency of the detector was determined by measuring resonances with very well known strengths and branchings. A typical γ spectrum of the ^{92}Mo$(\alpha,\gamma)^{96}$Ru reaction taken at the alpha-beam energy of 10 MeV is shown in Fig. 1.

Table 1
List of reactions studied in the present work.

Reaction	Energy range E_α (MeV)	Target Thickness ($\mu g/cm^2$)	Target Enrichment (%)	Target material form
^{92}Mo$(\alpha,\gamma)^{96}$Ru	8.0 - 11.0	398	92.8	Metallic
^{91}Zr$(\alpha,\gamma)^{95}$Mo	9.5 - 11.5	930	89.9	Metallic
^{92}Zr$(\alpha,\gamma)^{96}$Mo	9.6 - 11.5	1390	95.13	Metallic
^{104}Pd$(\alpha,\gamma)^{108}$Cd	9.5 - 11.5	607	91.2	Metallic
^{116}Sn$(\alpha,\gamma)^{120}$Te	9.5 - 11.3	863	96.3	$^{116}SnO_2$
^{118}Sn$(\alpha,\gamma)^{122}$Te	10.5 - 11.7	1700	98.8	Metallic

3 Data analysis

In order to obtain the cross section of an (α, γ) reaction one has to determine the absolute number of final nuclei produced. These de-excite through γ-ray emmission. Such de-excitations proceed either through the emmission of a single γ-ray directly to the ground state (γ_0 transition), or through γ cascades populating various intermediate levels before eventually feeding the ground state. In the case of the 4π calorimeter, sequential γ-transitions are summed, thus resulting in the so-called sum peak, which is located at the energy $E_{\gamma_0} = E_{c.m} + Q$, where Q is the Q-value of the reaction. A typical sum peak is shown in Fig.1. As can be seen there, the beam-induced background below the sum peak is negligible: By determining the area Y under the sum peak, one obtains the cross section σ_T of the reaction from:

$$\sigma_T = \frac{A \cdot Y}{N_A \cdot \xi \cdot \varepsilon \cdot N_B} \tag{1}$$

where A is the atomic weight of the target nucleus, N_A is the Avogadro number, ξ is the target (areal) thickness, ε is the detector efficiency at the corresponding γ-ray energy and N_B is the total number of incident particles.

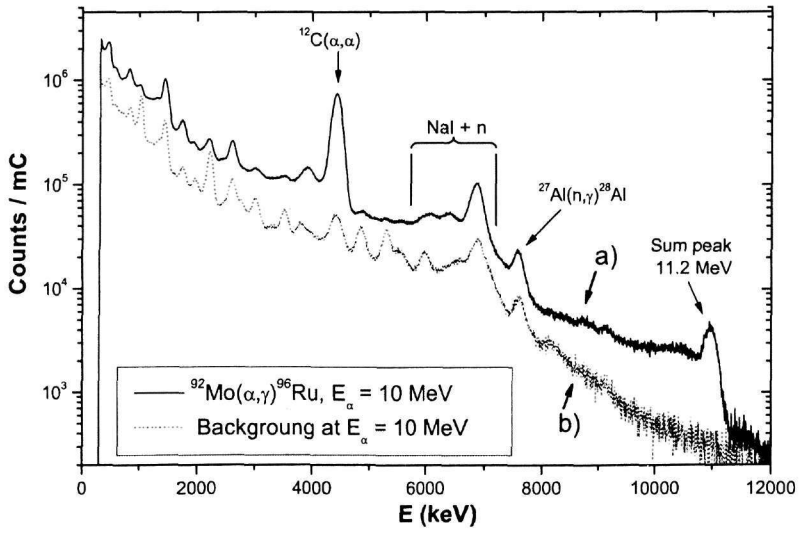

Fig. 1. *a) Gamma spectrum of the $^{92}Mo(\alpha,\gamma)^{96}Ru$ reaction taken at $E_\alpha = 10$ MeV. b) Beam induced background spectrum at the same beam energy.*

4 Comparison with theory

Theoretical cross sections were obtained with the statistical-model code MOST [2]. Different combinations of nuclear parameters such as Nuclear Level Densities (NLDs), nucleon-nucleus Optical Model Potentials (N-OMPs) and α-nucleus OMPs (α-OMPs) were used. In figure 2, the data of the $^{92}Mo(\alpha,\gamma)^{96}Ru$ reaction, which are plotted as black circles, are compared with the corresponding theoretical calculations, while figure 3 presents the same results for the case of the $^{104}Pd(\alpha,\gamma)^{108}$ reaction. In figure 2, the solid curves correspond to different α-OMPs, with the other nuclear input parameters being fixed. More specifically, the grey, light grey and black curves correspond to the three semi-microscopic potentials (I, II, III) of Demetriou *et al.* [5]. These three potentials include a microscopic real part, and different phenomenological parameterizations for the imaginary part of the OMP. In detail, OMP-I includes only a volume imaginary term, OMP-II includes both volume and surface imaginary terms, while OMP-III includes both volume and surface imaginary terms, and also dispersive corrections. In addition, four theoretical curves corresponding to different combinations of N-OMP and NLDs, but with the α-OMP fixed (OMP-III) are also presented in the same plot. The solid black line, short-dotted line and dotted line, use the microscopic potential of Jeukenne *et al.* (JLM) [6] combined with the NLDs of Goriely [7], Thielemann *et al.* [8]

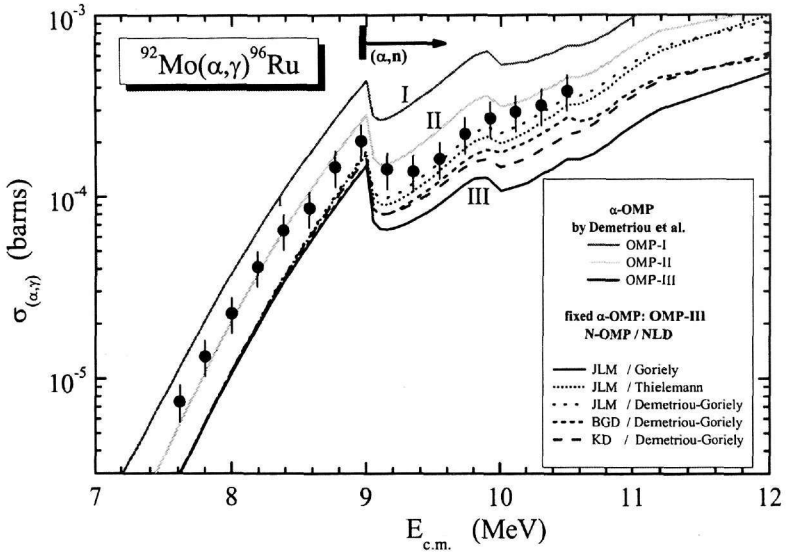

Fig. 2. *Cross sections (solid circles) measured for the $^{92}Mo(\alpha,\gamma)^{96}Ru$ reaction and theoretical HF calculations (curves). See also text.*

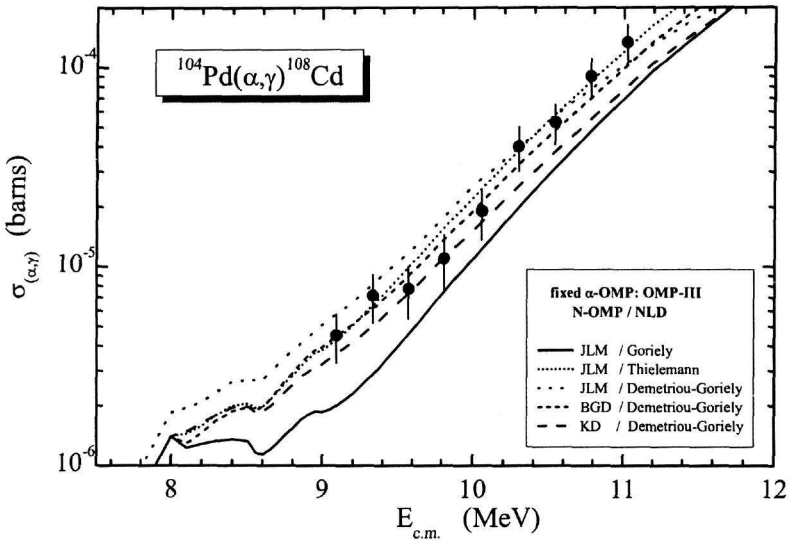

Fig. 3. *Cross sections (solid circles) measured for the $^{104}Pd(\alpha,\gamma)^{108}Cd$ reaction and theoretical HF calculations (curves). See also text.*

and Demetriou and Goriely [9], respectively. The latter NLDs are also combined with the phenomenological OMPs of Koning and Delaroche (KD) [10] (dash) and the semi-microscopic OMP of Bauge *et al.* (BGD) [11] (short-dash). Acording to this figure it is clear that the α-OMP II by [5] can reproduce the experimental data in a satisfactory way throughout the energy region. Using OMP III with different N-OMPs and NLDs also leads to a good description of the experimental data in the energy region above the neutron threshold, but it fails at lower energies, where the predictions are more sensitive to the α-OMP.

In the case of the $^{104}Pd(\alpha,\gamma)^{108}Cd$ reaction, presented in figure 3, the five curves correspond to the same combinations of N-OMPs and NLDs as described previously for the $^{92}Mo(\alpha,\gamma)^{96}Ru$ reaction, with the α-OMP III fixed. In this case, although the experimental data are reproduced by all the combinations used, the measurements are above the neutron threshold, and thus not very sensitive for distinguishing between the various α-OMPs. Similar results were obtained for the other reactions studied.

References

[1] M. Arnould, and S. Goriely, Phys. Rep. **384**, 1 (2003).

[2] S. Goriely, in Nuclei in the Cosmos V, edited by N. Prantzos and S. Harissopulos, (Edition Frontiéres, Paris, 1998), p. 314, (see also http://www-astro.ulb.ac.be).

[3] N. Piel *et al.*, Nucl. Instr. Meth. **B118** 186(1996).

[4] M. Mehrhoff *et al.*, Nucl. Instr. Meth. **B132** 671(1997).

[5] P. Demetriou, C. Grama, and S. Goriely, Nucl. Phys. **A707**, 253 (2002)

[6] J. P. Jeukenne *et al.*, Phys. Rev. **C16**, 80 (1977)

[7] S. Goriely, in "Nuclear Data for Science and Technology", Tsukuba, 7-12 October 2001, J. Nucl. Sci. Tech., supp. 2, vol 1, 536 (2002).

[8] F.K. Thielemann, M. Arnould, and J.W. Truran, Advances in Nuclear Astrophysics (Gif-sur-Yvette: Editions Frontiéres) p 525 (1986)

[9] P. Demetriou and S. Goriely, Nucl. Phys. **A695**, 95 (2001)

[10] A. Koning and J. Delaroche, Nucl. Phys. **A713**, 231 (2003)

[11] E. Bauge, J. P. Delaroche, and M. Girod, Phys. Rev **C63**, 24607 (2001)